

Development of a mobile solar air cooler with a clay-based cool water reservoir

Abstract - This study presents the design, simulation in SolidWorks and experimental validation of a mobile solar air cooler using clay as the base material. Faced with the challenges of climate change and limited access to conventional air conditioning in developing countries, this system offers an energy-autonomous and economically viable alternative. The methodology includes a literature review, multi-physics thermal modelling coupling heat transfer in porous media and fluid dynamics, the optimal choice of components (clay, 145.39 Wp photovoltaic panel, 50 Ah battery, fan) and the experimental characterisation of the prototype. Simulations were used to optimise the geometry and predict thermal distributions. The experimental results show a temperature reduction of 5°C (indoor temperature of 25°C for 30°C outdoors) with a relative humidity of 55%, an autonomy of two (02) days and a daily consumption of 537.6 Wh.

Keywords: *Evaporative cooling; Clay; Simulation; Thermal comfort.*

1. Introduction

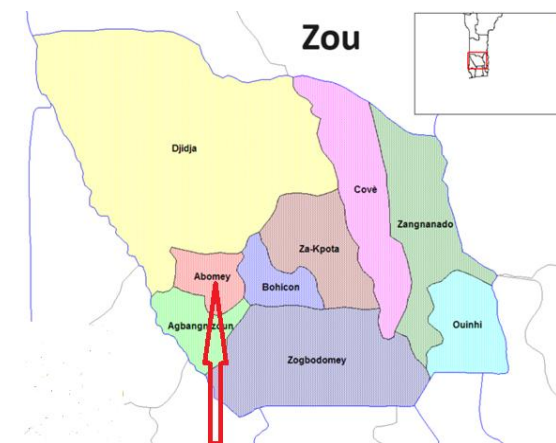
The steady rise in global temperatures, exacerbated by climate change, has increased demand for air conditioning systems, particularly in tropical and subtropical regions (T.F. Ishugah et al, 2024). This growing demand poses major challenges, especially in developing countries where access to electricity remains limited and energy costs represent a significant economic constraint. In sub-Saharan Africa, where temperatures can exceed 40°C for long periods, conventional cooling solutions remain largely inaccessible to a large part of the population (R. Lufu et al, 2025). In response to these challenges, evaporative cooling technologies using local materials and renewable energy are emerging as promising alternatives. These systems, based on the physical principle of water evaporation to absorb latent heat, have the advantage of being economically affordable and energy sustainable (T.S. Workneh, 2010). Recent research has demonstrated the effectiveness of these technologies in various applications, ranging from food preservation to building air conditioning (L. Xu et al, 2022). The use of clay as a base material for evaporative cooling systems has been the subject of growing interest in scientific literature. The intrinsic properties of clay, including its high porosity, water retention capacity and local availability, make it a particularly suitable material for passive cooling applications (D.P. Mondal et al, 2009). Recent studies have shown that water-saturated porous clay structures can significantly reduce ambient temperature, with particularly remarkable performance in hot and dry climates (G.A. Mustafa et al, 2025). The integration of solar energy into evaporative cooling systems represents an innovative approach that combines environmental sustainability and energy efficiency. Research conducted by S. Singhal (2021) has demonstrated the technical feasibility of solar-powered evaporative cooling systems, paving the way for autonomous solutions suitable for regions with high levels of sunshine (S. Singhal, 2021). This approach is particularly relevant for Africa, where solar radiation is abundant throughout the year. Experiments conducted in different African regions have confirmed the potential of cooling technologies using local materials. Studies conducted in the Sahel have highlighted the promising performance of photovoltaic systems coupled with evaporative cooling using local plant materials (E.M.S. El-Said et al, 2024). However, a critical analysis of the literature reveals certain gaps in existing research. Although many studies have explored the use of clay in static cooling applications, few have focused on the development of mobile systems incorporating a fresh water reservoir. Yet this mobility is a considerable advantage for small-scale residential and commercial applications, allowing flexible adaptation to specific user needs. Furthermore, most existing studies focus on specific applications such as food preservation (pot-in-pot systems) or photovoltaic panel cooling, without fully exploring the potential of clay systems for air conditioning living spaces. Recent work by S.O. Oyedepo et al(2021) on the experimental analysis of evaporative cooling of water in porous clay containers provides a solid foundation, but needs to be extended to air conditioning applications (S.O. Oyedepo et al, 2021). This study aims to fill these gaps by proposing the design and construction of a mobile solar air cooler with a clay-based cool water reservoir, specifically adapted to the climatic conditions and socio-economic constraints of developing countries such as Benin. The originality of this approach lies in the synergistic integration of three key elements: the use of local clay as the base material, the incorporation of a water pre-cooling system through storage, and the mobility of the device for flexible use.

38 **2. Materials and methods**

39 This section presents the equipment and materials used to build the air cooler, the research methodology and
40 the associated sizing. The main objective of this research is to develop an accessible, sustainable and effective
41 technological solution to improve thermal comfort in enclosed spaces, while promoting local resources and
42 renewable energies.

43 **2.1. Presentation of the study area**

44 Located in the centre of Benin, the commune of Abomey is the capital of the department of Zou. It has seven
45 (07) districts, including the district of Djegbe. Within the latter, there are several villages/city districts, notably
46 the Sogbo-Aliho district, where the Abomey University Centre (the subject of our study) of the National
47 University of Science, Technology, Engineering and Mathematics (UNSTIM) is located, not far from the Sogbo-
48 Aliho crossroads opposite the Sino-Beninese secondary school.



50
51
52
53
54
55
56 *Figure 1: Map showing the location of the municipality of Abomey*

57
58
59
60
61
62 **2.2. Equipment/materials used**

63 The equipment and measuring devices used during the design phase are described below:

64
65 *Table 2: List of equipment/materials*

Equipment/Material	Technical specifications
Clay canaries	<ul style="list-style-type: none">○ Apparent density: 1800-2200 kg/m³○ Porosity: 25-45% (microporous structure)○ Water permeability: 1×10^{-12} to 1×10^{-10} m²○ Thermal conductivity: 0.8-1.5 W/(m·K)○ Specific heat capacity: 800-1000

66		J/(kg·K)
67		<ul style="list-style-type: none"> ○ Water retention coefficient: High (absorption up to 20-30% of its weight)
68		
69		
70		<ul style="list-style-type: none"> ○ Model: Mist marker ○ Nominal voltage: 24 V ○ Nominal current: 1 A ○ Water flow rate: 250 ml/h ○ Temperature range: 5°C – 45°C ○ Ceramic membrane size: 16 mm
71	Mist marker	
72		
73		
74		
75		<ul style="list-style-type: none"> ○ Diameter: 12 cm ○ Rotation speed: 800 rpm ○ Maximum airflow: 43 cfm ○ Maximum air pressure: 1 mmH2O ○ Bearing type: Fluid bearing
76	Fan	
77		
78		
79		
80	Casing	<ul style="list-style-type: none"> ○ Materials: wood ○ Dimensions: 40 * 40 * 50 cm³

91 The funnel and T-shaped pipe served as ducts for the air flow outlet in our design. In addition, thermal and fluid
 92 modelling of the system was carried out using SOLIDWORKS CAD software, a parametric 3D mechanical
 93 design application that allows designers to quickly sketch ideas, experiment with features and dimensions, and
 94 produce accurate models and drawings. It is used to design and simulate models of the building and the clay
 95 device. Microsoft Excel, a spreadsheet application in the Microsoft Office suite, offers calculation, graphing, data
 96 analysis, and programming functions via VBA. Here, it enabled us to process monthly temperature and relative
 97 humidity data for the study area.

98 **2.3. Heat balance in the cooking stove**

99 To achieve our objectives, we followed a methodical approach based on modelling the cooling system in
 100 SolidWorks with a case study to experimentally validate the results.

101 **2.3.1. Operating principle**

102 The mobile solar air cooler with a clay water tank works on the simple and natural principle of evaporative
 103 cooling. The device consists mainly of a clay tank filled with water, a misting system, and a solar-powered fan.
 104 Through capillary action, the clay causes a thin layer of water to migrate to its surface, where it evaporates under
 105 the effect of ambient heat: this endothermic process draws heat from the reservoir and the adjacent air, causing
 106 them to cool. At the same time, the misting system disperses micro-droplets into the air flow; the rapid
 107 evaporation of these droplets enhances heat transfer and increases cooling efficiency. The fan draws in warm
 108 outside air and sends it to the cooling zone (reservoir + misting system), so that the expelled air is cooler and
 109 slightly humidified. This synergy between natural evaporation, misting and solar ventilation lowers the indoor
 110 temperature by several degrees.

111 **2.3.2. Specifications**

112 Our project aims to create a mobile, energy-efficient air cooler that can cool the ambient air in areas without
 113 constant access to electricity, using local materials such as clay. The following considerations have been made:

- 114 ○ Type of room to be cooled: an office measuring L=3m; l= 3m and h =2.5 m
- 115 ○ Average outside temperature: 30°C.
- 116 ○ Outdoor relative humidity: 45%.
- 117 ○ Target indoor temperature: 24°C.
- 118 ○ Target relative humidity: 55%.
- 119 ○ System operating time: 8 hours per day.
- 120 ○ Air density: $\rho = 1.20 \text{ kg/m}^3$
- 121 ○ Specific heat of air: 1.005 kJ/kg.K
- 122 ○ Water source: clay jugs with a capacity of 2 L.
- 123 ○ Latent heat of vaporisation $\Delta H = 2500 \text{ kJ/kg}$
- 124 ○ Number of lamps used for lighting: 1 lamp
- 125 ○ Amount of heat emitted by the lamp: 16 W
- 126 ○ Amount of heat emitted by the computer: 250W
- 127 ○ Amount of heat emitted by the occupant (sensible gains): 67W

128

129 **2.4. Sizing**

130 **2.4.1. Amount of heat to be removed**

131 The amount of heat that the cooling system must overcome can be estimated using the formula:

$$132 \quad Q_T = Q_L + Q_{OC} + Q_{OR} \quad (1)$$

- 133 - Q_T : Amount of heat to be removed (W)
- 134 - Q_L : Amount of heat emitted by the lamp (W)
- 135 - Q_{OC} : Amount of heat emitted by the occupant (W)
- 135 - Q_{OR} : Amount of heat emitted by the computer (W)

136 **2.4.2. Volume of the room to be cooled**

137 The volume of the room to be cooled is calculated using the following formula:

$$138 \quad V_{ch} = L * l * H \quad (2)$$

- 139 - L : Length of the room in metres (m)
- 140 - l : Width of the room in metres (m)
- 141 - H : Height of the room in metres (m)

142 **2.4.3. Mass flow rate of evaporated water**

143 The formula opposite allows us to find the mass flow rate:

$$144 \quad q_m = \rho_e * q_v \quad (3)$$

- 145 - q_m : Mass flow rate of evaporated water ($\text{kg} \cdot \text{s}^{-1}$)
- 146 - q_v : Volumetric flow rate of water ($\text{m}^3 \cdot \text{s}^{-1}$)
- 147 - ρ_e : Density of water ($\text{kg} \cdot \text{m}^{-3}$)

149 **2.4.4. Cooling capacity**

150 The cooling capacity of the system is calculated using the following formula:

$$151 \quad P_f = q_m * L_v + q_{ma} * C_p * \Delta T \quad (4)$$

- 151 - P_f : Cooling capacity (W)
- 152 - q_m : mass flow rate of evaporated water ($\text{kg} \cdot \text{s}^{-1}$)
- 153 - L_v : latent heat of vaporisation of water ($\text{kJ} \cdot \text{kg}^{-1}$)
- 154 - q_{ma} : air mass flow rate ($\text{kg} \cdot \text{s}^{-1}$)

155 - C_p : specific heat of air (kJ/kg.K)
 156 - ΔT : Temperature difference (K)

157 **2.4.5. Sizing the power supply system**

158 The sizing of a photovoltaic system begins with an assessment of solar energy requirements.

159 ○ **Electrical energy requirements**

160 This requirement can be determined using the following formula:

$$E_c = \sum_{i=1}^n P_i * t_i \quad (5)$$

162 - E_c : Electrical energy consumed (Wh)
 163 - P_i : Power of equipment i (W)
 164 - t_i : Operating time of equipment i (seconds)
 165 - n : Number of pieces of equipment in the building

166 ○ **Choice of panels**

167 ✓ **Peak power**

168 The peak power of the installation to be used is given by the following expression:

$$P_c = \frac{E_b}{I_r \times k} \quad (6)$$

171 - P_c : Peak power of the field in Wc;
 172 - k : Cumulative coefficient of losses due to voltage and conversion , $k= 0.65$;
 173 - I_r : Solar radiation received on 1 m² in Wh/m²/day, $I_r = 5$ Wh/m²/jour in southern Benin.

174 ✓ **Number of panels to be installed**

175 The number of panels N_p is given by the following formula:

$$N_p = \frac{P_c}{P_{cu}} \quad (7)$$

176 P_{cu} : Peak power of a panel in (Wp)

177 ✓ **Number of panels in series**

178 The number of N_{ps} panels to be connected in series is given by the formula:

$$N_{ps} = \frac{\text{system voltage}}{\text{Rated panel voltage}} \quad (8)$$

179 The voltage of the photovoltaic system is chosen according to the power of the PV field.

180 ✓ **Number of strings**

181 The number of panels to be connected in parallel N_{pp} is given by the following formula:

$$N_{pp} = \frac{\text{number of panels}}{\text{Number of panels in series}} \quad (9)$$

182 ○ **Choice of batteries**

183 The capacity of the battery bank C_b is calculated using the formula below:

$$C_b = \frac{E_c \times N_j}{U_s \times DOD \times \eta_b} \quad (10)$$

184 - E_c : energy requirement consumed in kWh;

191 - N_f : desired number of days of autonomy in days;
 192 - U_s : system voltage in V;
 193 - DOD : deep discharge rate of the battery.
 194 - η_b : battery efficiency. Either 0.7 or 0.9 is used as the efficiency, depending on the battery used.
 195

196 ○ **Choice of charge controller**

197 The sizing carried out here concerns a PWM (Pulse Width Modulation) regulator due to its low cost. To size
 198 a charge regulator, it is essential to know two main parameters: the system voltage and the total short-circuit
 199 current of the PV solar field.

200
$$I_{cct} = 1,25 \times I_{cc} \times N_{pp} \#(11)$$

201 - I_{cct} : total short-circuit current of the PV solar field;
 202 - I_{cc} : short-circuit current of a PV solar module;
 203 - N_{pp} : number of panels in parallel

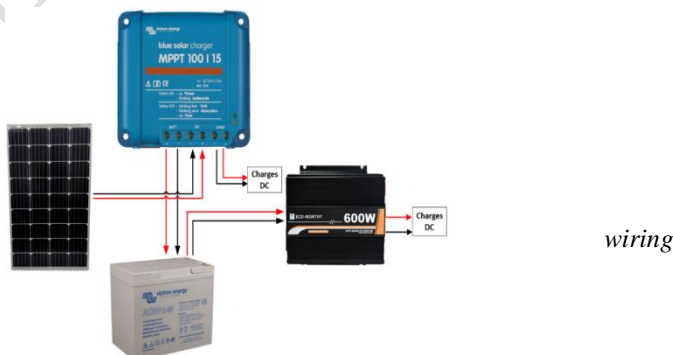
204 ○ **Choosing an inverter**

205 The power of the inverter is given by the following formula:

$$P_o = \frac{k \times P_t}{\eta_o} \#(12)$$

207 - P_o : Power of the inverter in (W);
 208 - P_t : Total load power in (W);
 209 - η_o : Inverter efficiency;
 210 - k : Reserve coefficient.

211 ○ **System wiring diagram**



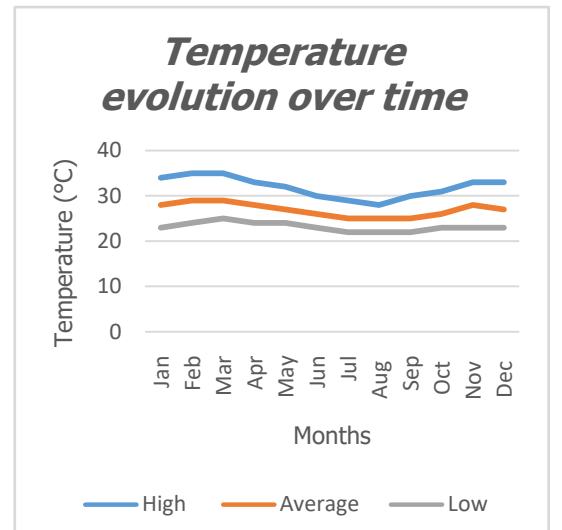
224 Figure 2: Photovoltaic system

225 3. Results and discussion

226 Modelling and numerical simulation of the mobile solar air cooler with a clay cool water reservoir were
 227 carried out using SolidWorks in order to analyse the thermo-fluidic behaviour of the device. The results obtained
 228 mainly concern the distribution of air temperature and current lines within the system.

229 3.1. Study area conditions

230 Figures 1 and 2 show the evolution of temperature and relative humidity over time, respectively.



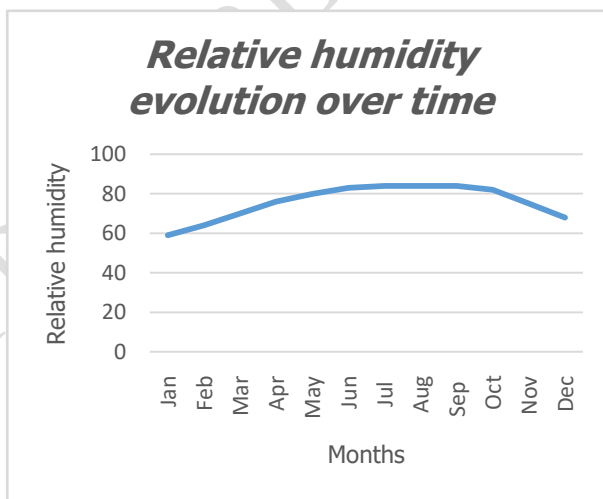
233
234 *Figure 3: Temperature change over time.*

235 The shape of the temperature curves shows the following trends:

- 236 ○ The high temperature varies between 28°C and 35°C, with a peak around February and March.
- 237 ○ The average temperature varies between 25°C and 29°C, with a relative low in July and August.
- 238 ○ The low temperature is fairly stable at around 22°C to 25°C throughout the year.

239 We note that the cooler must be able to effectively manage temperatures around 30 to 35°C during the dry
240 season while remaining efficient and stable for lower and average temperatures throughout the year.

241



242 *Figure 4: Change in relative humidity over time*

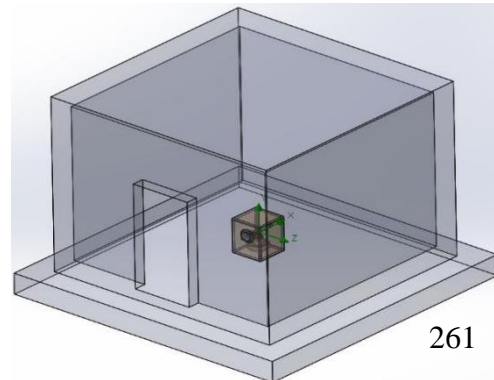
243 From the figure 4, it can be noticed that:

- 244 ○ Relative humidity is 60% at the beginning of the year (November–February: dry season). This creates
245 favourable conditions for evaporation.
- 246 ○ Relative humidity increases to ~82–85% in the middle of the year (June–August: peak of the wet
247 season). This creates conditions that are not conducive to direct evaporation.
- 248 ○ Relative humidity then decreases (September–October: return to the dry season).

249 The performance of the device must therefore be highly seasonal: effective in the dry season and limited in
250 the rainy season.

251 **3.2. 3D models of the building and the cooling device**

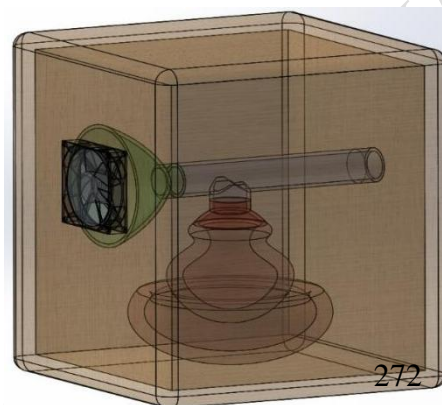
252 Figures 5, 6 and 7 show 3D models of the building and the designed device.



261 *Figure 5: 3D model of the*

261

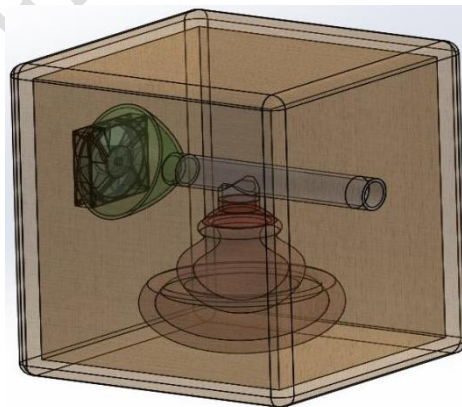
building



272 *Figure 6: 3D model of the*

272

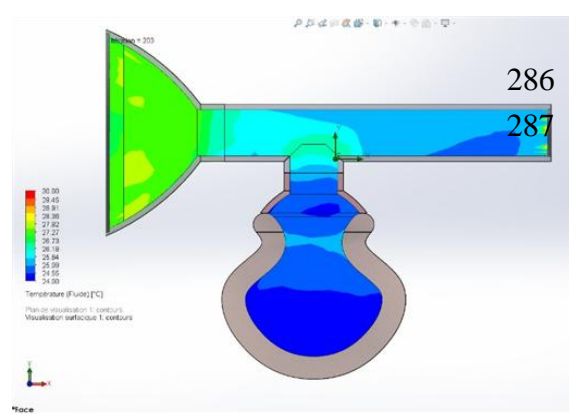
device: front view



283 *Figure 7: 3D model of the device: rear view*

286 **3.3. Simulation**

287 In Figure 8 shows
288 simulation of the device.



286 **results**

287 the result obtained from the

251

252

253

254

255

256

257

258

259

260

261

262

263

264

265

266

267

268

269

270

271

272

273

274

275

276

277

278

279

280

281

282

283

284

285

286

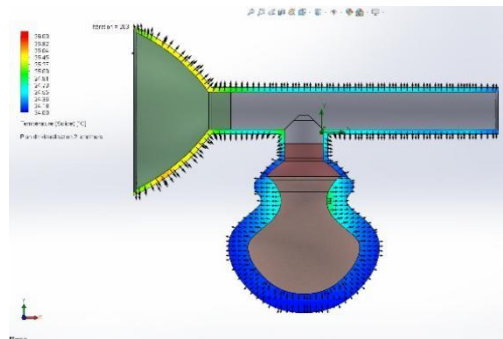
287

288

289

290
291
292
293
294
295
296
297

298 *Figure 8: Thermal simulation of the device*

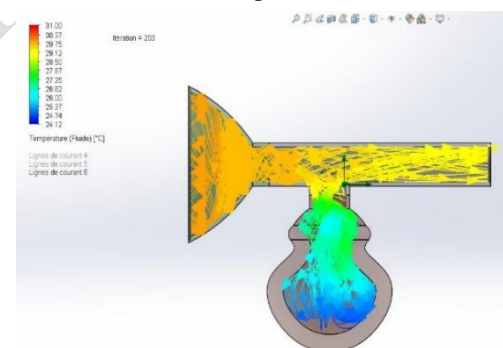


300
301
302
303
304
305
306
307 *Figure 9: Contour simulation of the device*

308 The results show that the temperature inside the clay canary is mainly between 24 and 25 °C, particularly in
309 the lower and central areas of the tank. This high prevalence of low temperatures, shown in dark blue, indicates
310 effective and stable cooling of the air in contact with the tank. On the other hand, the upper part of the canary and
311 the transition zone to the T-shaped duct have slightly higher temperatures, reaching 28 to 29 °C. Similarly, the
312 air circulating in the horizontal duct initially maintains a higher temperature, close to 29 °C, corresponding to the
313 air entering the device.

314 This thermal distribution reveals the existence of a significant temperature gradient between the air duct and
315 the clay reservoir, reflecting a gradual heat transfer from the warm air to the cooling wall of the canary.

316 Similar results were reported by F. Wang et al (2017), who showed that air circulating near water-saturated
317 porous clay tubes undergoes a significant decrease in temperature due to heat transfer and evaporation through
318 the porous walls.

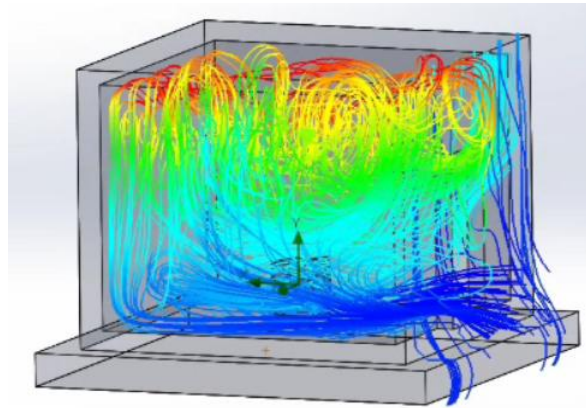


319
320
321
322
323
324
325
326 *Figure 10: Thermal simulation of current lines at the device's*

327 Analysis of the streamlines reveals a steady flow of air from the inlet duct to the reservoir. Warm air from the
328 room first enters the T-shaped section and is then gradually cooled as it passes into contact with the internal
329 walls of the canary.

330 The thermal stratification observed, with colder air concentrated in the lower part of the tank, can be
331 explained by the higher density of the cooled air and the low level of turbulence inside the canary. This
332 behaviour is characteristic of a passive thermal tank, promoting cooling stability over time. This is precisely
333 what Figure 11 shows when the device is simulated inside a building.

334
335
336
337
338
339
340
341
342
343



344 *Figure 11: Thermal simulation of current lines at building level*

345 The simulation results show that the device is capable of producing cooled air at a temperature of around
346 24°C, which is particularly interesting for areas with a hot climate. The temperature difference observed between
347 the incoming air and the cooled air highlights the real potential of the system for passive cooling of buildings.

348 However, the persistence of higher temperature zones in the T-shaped section suggests that cooling is limited by
349 the air-clay contact time, an aspect also highlighted in the literature as a key parameter influencing the thermal
350 performance of passive coolers (J.S. Reed, 1995). These results indicate that geometric optimisation of the
351 device could lead to further performance improvements.

352 **3.4. Experimentation**

353 **3.4.1. Prototype of the device**

354 A physical prototype of the system was built, as shown in Figure 12, and was subjected to experiments.



366 *Figure 12: Physical prototype of the device*

367

368 **3.4.2. Testing under real conditions**

369 After the air cooler was built, a commissioning and testing phase was carried out. It was observed that the
370 device gradually lowered the temperature of the room shortly after being switched on. The temperature dropped
371 from 29 °C to around 25 °C. However, the desired temperature of 24 °C could not be reached. The temperature
372 stagnated at 25°C. This seems to be mainly related to the geometry of the T-shaped part of the device.



386 *Figure 13: Test under real conditions on the device*

373
374
375
376
377
378
379
380
381
382
383
384
385
386
387

388 3.5. Influence of thickness

389 TheTable 2 below summarises these cost estimates.

390

Table 2: Estimated cost of producing the module.

Description	Quantity	Total cost (FCFA)
Box	1	20,000
Canaries	2	500
Fan	1	5,000
Mist sprayer	1	12,000
Photovoltaic panel	1	25,000
Battery		12,000
Labour	1	20,000
	-	
Other	-	3,200
Total		98,500

391

392 The cost of construction is estimated based on the cost of components, materials and labour.The prices
393 shown in Table 2 are based on local market rates. It is important to note that these rates may be subject to
394 fluctuations depending on the supplier or subject to VAT.The total estimated cost of producing the control
395 module is 98,000 CFA francs.

396 The results of our experiments indicate that the device shows promise in terms of efficiency and quality.
397 However, further investigation is needed to explore other avenues such as automatic cooling control and
398 geometric optimisation of the T-shaped part of the device .

399

400 4. Conclusion

401 This article proposed a mobile, economical and environmentally friendly cooling solution suitable for areas
402 withhigh temperatures and low access to electricity. The cooler developed is based on the principle of direct
403 adiabatic evaporation, where water absorbed into the clay wall evaporates on contact with hot air, causing a
404 significant drop in temperature (30 to 24 °C). The choice of local materials such as clay, combined with a low-
405 voltage ventilation system and a misting device, has made it possible to achieve satisfactory thermal

406 performance, with an airflow temperature close to 24°C in ambient conditions of 30 to 35°C, as confirmed by
407 numerical simulations.

408 Overall, the device effectively meets expectations; however, future improvements could make it even more
409 efficient. Indeed, the geometric optimisation of the T-shaped part of the device and the addition of a regulation
410 system to better control ambient conditions are all prospects that will make the device more efficient and
411 attractive.

412 Acknowledgements

413 Many thanks to all those who contributed to this work through their comments and suggestions.

414 Declaration of competing interests

415 The authors declare that they have no known competing financial interests or personal relationships that
416 could have appeared to influence the work reported in this paper.

417 References

418 E. M. S.El-Said, G. B.Abdelaziz, A. Y. Al-Zubaydi, M. I. M.Abdelhady, N.Shokry, S.Mohamed and M.
419 A.Dahab (2024), Experimental investigation of earth-air heat exchanger using porous clay vessels for eco-
420 friendly buildings,*Scientific Reports*, 14, 17548. <https://doi.org/10.1038/s41598-024-67212-5>

421 T. F.Ishugah, J. Kiplagat, J. Madete andJ. Musango(2024), Current status, challenges, and opportunities of
422 evaporative cooling for building indoor thermal comfort using water as a refrigerant: A review,*International
423 Journal of Energy Research*, 26, 1026136. <https://doi.org/10.1155/2024/1026136>

424 R. Lufu, A. Ambaw andL.U. Opara(2025), Evaporative cooling systems for perishables in Sub-Saharan
425 Africa—A review,*Journal of Food Process Engineering*, 48(5), e70127. <https://doi.org/10.1111/jfpe.70127>

426 D. P.Mondal, S. Das, A. Badkul andN. Jha (2009),*Modelling of evaporative cooling of porous medium filled
427 with evaporative liquid*, Computers, Materials & Continua, 13(2), 115–134.
<https://doi.org/10.3970/cmc.2009.013.115> .

428 G. A.Mustafa, H. Hamdy andA.N. Sameh (2025), Parametric analysis of water-saturated porous clay
429 structures as evaporative cooling of building integrated photovoltaic systems,*Energy*, 320, 135471.
<https://doi.org/10.1016/j.energy.2025.135471>

430 S.O. Oyedepo, O.S.IFayomi, J.O. Dirisu, U.K. Efemwenkiekie and A. Arhagba(2021),*Experimental
431 Analysis of Evaporative Cooling Water inPorous Clay Vessels Under Varying Ambient Conditions*,Materials
432 Science and Engineering 1107 (2021) 012103. Doi:10.1088/1757-899X/1107/1/012103

433 J.S. Reed (1995),Introduction to the principles of ceramic processing, Wiley, 2nd Ed.
<https://doi.org/10.1016/j.applthermaleng.2024.125269>

434 S. Singhal (2021), Solar powered incabin evaporative cooling system,*SAE Technical Paper* 2021-280144.
<https://doi.org/10.4271/2021-28-0144>

435 F. Wang,T. Sun, X. Huang, Y. Chen and H. Yang (2017),*Experimental research on a novel porous ceramic
436 tube type indirect evaporative cooler*,Applied Thermal Engineering, 24, 1191–1199.
<https://doi.org/10.1016/j.applthermaleng.2017.07.111>

437 T. S.Workneh (2010), Feasibility and economic evaluation of low-cost evaporative cooling system in fruit
438 and vegetables storage,*African Journal of Food, Agriculture, Nutrition and Development*, 10(8), 2984–2997.
439 DOI: [10.4314/ajfand.v10i8.60885](https://doi.org/10.4314/ajfand.v10i8.60885)

440 L. Xu, D.W. Sun, Y. Tian, L. Sun, T. Fan and Z. Zhu (2022), Combined effects of radiative and evaporative
441 cooling on fruit preservation under solar radiation: Sunburn resistance and temperature stabilisation,*ACS Applied
442 Materials and Interfaces*, 14(40), 45788–45799. <https://pubs.acs.org/doi/10.1021/acsami.2c11349>

443

444

445

446

447

448

449